

TIFR/TH/00-23

SHEP/00-07

hep-ph/0006198

Does LEP prefer the NMSSM?

M. Bastero-Gil¹, C. Hugonie², S. F. King¹, D. P. Roy³, S. Vempati⁴

¹*Department of Physics and Astronomy, University of Southampton,
Southampton, SO17 1BJ, U.K.*

²*Rutherford Appleton Laboratory,
Chilton, Didcot, Oxon, OX11 0QX, U.K.*

³*Theoretical Physics Department, Tata Institute of Fundamental Research,
Homi Bhabha Road, Bombay 400 005, India*

⁴*Theory Group, Physical Research Laboratory,
Navarangpura, Ahmedabad 380 009, India.*

Abstract

We study the naturalness of electroweak symmetry breaking and baryogenesis in the next-to-minimal supersymmetric standard model (NMSSM). Our study is motivated by the recent LEP bounds on the Higgs boson mass which severely constrains the low $\tan \beta$ region of the minimal supersymmetric standard model (MSSM). We show that the low $\tan \beta$ region of the NMSSM is clearly favoured over the MSSM with regard to the physical Higgs boson mass, fine-tuning, and electroweak baryogenesis.

1 Introduction

The latest LEP bound on the Standard Model like Higgs boson mass m_h is in the region of $m_h > 108$ GeV once the limits from all the experiments are combined [1]. Such a bound on the Higgs mass can be interpreted as the lightest scalar Higgs mass bound of $m_h > 105$ GeV in the low $\tan \beta (\leq 4)$ region of the minimal supersymmetric standard model (MSSM). Such a large Higgs mass implies large fine-tuning in the low $\tan \beta$ region [2], and leads to the smallest values of $\tan \beta$ being excluded. This is disturbing since electroweak baryogenesis in the MSSM relies on low $\tan \beta$ and light Higgs and stop masses [3] ¹.

It is well known that in the next-to-minimal supersymmetric standard model (NMSSM) [5] the lightest Higgs boson can be heavier than in the MSSM [6]. It is also well known that the parameter space for electroweak baryogenesis in the NMSSM is much larger than in the MSSM, due to trilinear contributions to the scalar potential at tree-level. What has not been realised so clearly is that these two features go together with low $\tan \beta$. This is a timely observation, given the constraints that LEP places on the MSSM in the low $\tan \beta$ region. Moreover, although fine-tuning has been well studied in the MSSM it has not been systematically studied in the NMSSM. In this letter, then, we compare the fine-tuning in the NMSSM and MSSM in the low $\tan \beta$ region and show that the NMSSM is much preferred. We then study the strength of the electroweak phase transition (EWPT) in the NMSSM, and show that, unlike in the MSSM, a sufficiently strong first order phase transition persists over much of the low $\tan \beta$ region.

Although the NMSSM provides a testable solution to the μ problem, by replacing the superpotential term $\mu H_1 H_2$ by $\lambda N H_1 H_2$ (where H_i are Higgs doublets and N is

¹When SUSY phases are included the parameter space for electroweak baryogenesis is somewhat increased, however [4].

a Higgs singlet) it is often criticised for leading to a conflict between cosmological domain walls and stability due to supergravity tadpoles. It has recently been pointed out, however, that the NMSSM remains a natural solution to the μ problem since both the stability and the cosmological domain wall problems may be eliminated by imposing a \mathbb{Z}_2 R-symmetry on the non-renormalisable operators [7]. Thus the NMSSM appears to be well motivated both theoretically and phenomenologically at the present time. Indeed the solution of the μ problem is closely linked to the two phenomenological features of NMSSM noted above in the sense that all the three originate from the same term in the superpotential, as we shall see below.

2 Fine-Tuning in the NMSSM

Although fine-tuning is not a well defined concept, the general notion of fine-tuning is unavoidable since it is the existence of fine-tuning problem in the standard model which provides the strongest motivation for low energy supersymmetry, and the widespread belief that superpartners should be found before or at the LHC. If one abandons the notion of fine-tuning then there is no reason to expect superpartners at the LHC. Although a precise measure of *absolute* fine-tuning is impossible, the idea of *relative* fine-tuning can be helpful in selecting certain models and regions of parameter space over others. It is useful to compare different models using a common definition of fine-tuning [8]

$$\Delta_a = \text{abs} \left(\frac{a}{M_Z^2} \frac{\partial M_Z^2}{\partial a} \right) \quad (1)$$

where a is an input parameter, and fine-tuning Δ^{\max} is defined to be the maximum of all the Δ_a . It is worth pointing out that at low values of $\tan \beta$ fine-tuning is worse in the MSSM for two separate reasons. First, the tree level contribution to the Higgs mass squared upper bound $M_Z^2 \cos^2 2\beta$ goes down; so that one must rely more on radiative corrections to meet the LEP bound, which demand a higher value of $M_3(0)$

as observed in [2]. Second, the top quark Yukawa coupling is larger for low values of $\tan\beta$, so the Higgs mass gets driven more negative, resulting in larger coefficients of the $M_3^2(0)$ term in eq. 1, which again increases fine-tuning. A quantitative study of fine-tuning reveals that it is the experimental limit on the Higgs mass rather than the gluino mass, that provides the most severe fine-tuning for low values of $\tan\beta$, as discussed in the second reference in [2]. Moreover the fine-tuning required in the MSSM increases exponentially with the Higgs mass, since the radiative corrections to the Higgs mass increase logarithmically with the stop masses, and the stop masses increase in proportion to $M_3(0)$ which controls the fine-tuning [2].

While the Higgs quartic coupling in the MSSM is related to the gauge couplings, in the NMSSM it has an additional contribution from the Yukawa coupling λ . Consequently the tree level mass limit of the lightest Higgs scalar gets modified to

$$m_h^2 \leq M_Z^2 \left(\cos^2 2\beta + \frac{2\lambda^2}{g^2 + g'^2} \sin^2 2\beta \right). \quad (2)$$

Note that the additional term in Eq.2 is most effective where its help is needed most, i.e. at low $\tan\beta$. Assuming this Yukawa coupling to remain perturbative up to the unification scale of $\sim 10^{16}$ GeV implies $\lambda \lesssim 0.7$ at the electroweak scale [6], i.e. a contribution of $\sim M_Z^2 \sin^2 2\beta$ to the tree level mass limit. On the other hand, the upper limit on the mass of the lightest CP even Higgs is not necessarily physically relevant, since its coupling to the Z boson can be very small. Actually, this phenomenon can also appear in the MSSM, if $\sin^2(\beta - \alpha)$ is small. However, the CP odd Higgs boson A is then necessarily light ($m_A \sim m_h < M_Z$ at tree level), and the process $Z \rightarrow hA$ can be used to cover this region of the parameter space in the MSSM. In the NMSSM, a small gauge boson coupling of the lightest CP even Higgs is usually related to a large singlet component, in which case no (strongly coupled) light CP odd Higgs boson is available. Hence, Higgs searches in the NMSSM have possibly to rely on the search for the second lightest Higgs scalar, which can be

substantially heavier [9]. In the limit that the singlet decouples, and is the heaviest scalar, the inequality in Eq.2 may be approximately saturated by the lightest Higgs boson. Alternatively if the singlet decouples, but is the lightest scalar, then the inequality in Eq.2 may be approximately saturated by the second lightest scalar, which is the physical Higgs boson. In fact this latter case applies to the results we present later in the figures. In all cases it is clear that the NMSSM does not require a large radiative correction to satisfy the Higgs mass limit from LEP. It is this modification of the Higgs sector in the NMSSM which is responsible for the opening up the low $\tan\beta$ region of parameter space in this model, by removing the connection between the Higgs mass and exponential increases in fine-tuning present in the MSSM.

The NMSSM superpotential is defined as

$$W = \lambda NH_1H_2 + \frac{k}{3}N^3 + \dots \quad (3)$$

where the elipsis stand for quark and lepton Yukawa couplings, and the Higgs potential is

$$\begin{aligned} V_{NMSSM} = & m_1^2 v_1^2 + m_2^2 v_2^2 - 2m_3^2 v_1 v_2 + \lambda^2 v_1^2 v_2^2 \\ & + \frac{1}{8}(g'^2 + g^2)(v_1^2 - v_2^2)^2 + x^2(m_N^2 + \frac{2}{3}kx A_k + k^2 x^2) \end{aligned} \quad (4)$$

where $v_i = \langle H_i \rangle$, $x = \langle N \rangle$ and

$$m_1^2 = m_{H_1}^2 + \lambda^2 x^2, \quad m_2^2 = m_{H_2}^2 + \lambda^2 x^2, \quad m_3^2 = -\lambda x(kx + A_\lambda). \quad (5)$$

A_λ, A_k are the trilinear soft parameters associated with the λ, k terms in the superpotential, which play a prominent role in ensuring a strong 1st order EWPT, as we shall see in the next section. One-loop corrections to the effective potential, $\Delta V^{(1)}$, are taken into account by redefining the scalar masses such that $m_i^2 \rightarrow m_i^2 + \partial \Delta V^{(1)} / \partial v_i^2$.

The NMSSM minimisation conditions are then

$$\frac{M_Z^2}{2} = \frac{m_2^2 - m_1^2 \tan^2 \beta}{\tan^2 \beta - 1}$$

$$\begin{aligned}
\sin 2\beta &= \frac{2m_3^2}{m_1^2 + m_2^2 + \lambda^2 v^2} \\
0 &= \lambda x(2kx + A_\lambda) \frac{v_1 v_2}{x^2} + kx(2kx + A_k) + (\lambda^2 v^2 + m_N^2)
\end{aligned} \tag{6}$$

The results in eq. 6 can then be used to derive a master formula for the derivative of the Z mass with respect to input parameters, from which one can obtain the sensitivity parameter in eq. 1

$$\begin{aligned}
\frac{\partial M_Z^2}{\partial a} &= \frac{2}{\tan^2 \beta - 1} \left\{ \frac{\partial m_1^2}{\partial a} - \tan^2 \beta \frac{\partial m_2^2}{\partial a} - \frac{\tan \beta}{\cos 2\beta} \left(1 + \frac{M_Z^2 - \lambda^2 v^2}{m_1^2 + m_2^2 + \lambda^2 v^2} \right) \right. \\
&\quad \times \left. \left[2 \frac{\partial m_3^2}{\partial a} - \sin 2\beta \left(\frac{\partial m_1^2}{\partial a} + \frac{\partial m_2^2}{\partial a} + \frac{\partial \lambda^2 v^2}{\partial a} \right) \right] \right\}.
\end{aligned} \tag{7}$$

This result is very similar to the master formula obtained in the MSSM, to which it reduces in the limit $\lambda \rightarrow 0$. Of course the partial derivatives on the right-hand side will be quite different since they bring in derivatives of λx rather than μ , and x is a function of all the soft parameters (unlike μ in the MSSM which is independent of the soft parameters.) Thus the implementation of the master formula in the NMSSM is more involved than in the MSSM. Nevertheless, the variation of the VEVs follows from the minimisation conditions of the potential, such that:

$$\frac{\partial^2 V_{NMSSM}}{\partial a \partial v_i^2} = 0, \quad \frac{\partial^2 V_{NMSSM}}{\partial a \partial x^2} = 0. \tag{8}$$

The above system of 3 coupled equations can then be solved for $\partial v_i / \partial a$, and $\partial x / \partial a$. The other partial derivatives we need to evaluate the master formula eq. 7, such as $\partial \lambda / \partial a$, $\partial m_{H_i}^2 / \partial a \dots$, are computed numerically when running the renormalisation group equations (RGEs).

The NMSSM minimisation conditions are clearly analogous to those of the MSSM, and they may be satisfied by an analogous procedure. In both models the soft parameters are chosen at the high energy scale. Once the (low energy) value of $\tan \beta$ is selected, the top mass fixes the low energy top Yukawa coupling². In the NMSSM

²We include only QCD corrections when converting pole mass to running mass at the m_Z scale.

the additional low energy values of λ and k are selected. Next, all the Yukawas are run up to the high energy scale. Then all the soft masses are run down to low energies and the value of x (the analogue of μ in the MSSM) is fixed by the first minimisation condition (up to an ambiguity in the signs), and the value of A_λ (the analogue of B in the MSSM) is fixed by the second minimisation condition. In the NMSSM it then only remains to satisfy the third minimisation condition. In general this requires an iterative process since it relies upon having chosen the correct values of A_k and m_N at high energies (and both these parameters must be fixed before all the soft masses can be run down). ³ The structure of the Higgs potential being more complicated in the NMSSM than in the MSSM, the minimisation conditions (6) do not guarantee that we sit at a local minimum rather than at a local maximum, in which case the lightest squared mass eigenvalue is negative. The acceptable regions of the low energy parameter space where the physical scalar squared masses are positive were mapped out by Elliott et al in [6], and may be straightforwardly be achieved by adjusting the high energy soft Higgs masses $m_{H_1}(0)$ and $m_{H_2}(0)$. We therefore take a common value m_0 at M_{GUT} for the squark and slepton masses, but allow the input Higgs masses to be different. Also, a positive squared Higgs mass spectrum is favoured when $A_k(M_Z)$ is small, so we have adjusted the initial value of $A_k(0)$ such that $A_k(M_Z) = 0$.

In figs. 1-3 we plot the maximum sensitivity parameter Δ^{max} as a function of the lightest physical Higgs mass for both the NMSSM and MSSM, for the values of $\tan\beta = 2, 3, 5$. In these plots we have taken $m_0 = 100$ GeV, $A_t(0) = 0$ GeV, and assumed high energy first and second gaugino masses given by $M_2(0) = M_1(0) = 500$

³In the limit that we neglect the λ and k contributions to the right-hand sides of RGEs, the RGEs for the soft masses $m_Q^2, m_U^2, m_{H_1}^2, m_{H_2}^2$ become identical to those in the MSSM, and that for A_λ becomes identical to that for the soft parameter B in the MSSM. Furthermore m_N , A_k and k do not run in this limit. In this limit the first two minimisation conditions are identical to those of the MSSM and the third can trivially be satisfied by using it to fix m_N at the end. Although we never make this approximation, it serves to emphasise that main differences between the NMSSM and the MSSM arise from the low energy Higgs potential and scalar mass squared matrix not from RG running.

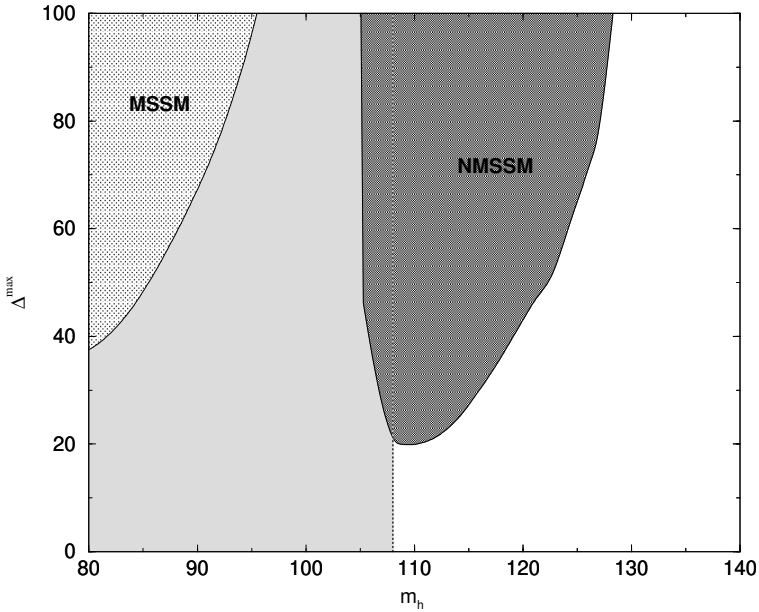


Figure 1: The maximum sensitivity parameter Δ^{max} as a function of the lightest physical Higgs mass for $\tan\beta = 2$. We have fixed $m_0 = 100$ GeV, $A_t(0) = 0$ GeV, $M_2(0) = M_1(0) = 500$ GeV and $\mu < 0$ ($\lambda x < 0$), while varying $M_3(0)$, $m_{H_1}(0)$ and $m_{H_2}(0)$. The darkest grey region correspond to the NMSSM, and the lighter grey region to the MSSM. The thin dotted line at 108 GeV, and the lightest shaded region to the left of it, represents the LEP excluded region on the standard model Higgs boson mass.

GeV. In our scans over parameter space we have restricted ourselves to $100 \text{ GeV} < M_3(0) < 600 \text{ GeV}$, $0 < m_{H_1}(0) < 1 \text{ TeV}$, and $\mu < 0$ ($\lambda x < 0$). In the MSSM, for each pair of points $(M_3(0), m_{H_1}(0))$ the upper limit on $m_{H_2}(0)$ is set by demanding the lightest chargino to be heavier than 90 GeV. For the NMSSM, we have taken $\lambda(0) = 1$ and $k(0) = -0.1$ as a sample point. The values of $A_\lambda(0)$ and $m_N(0)$ are obtained from the minimisation conditions, and we have restricted the range in $m_{H_2}(0)$ to those values which give rise to a physical Higgs spectrum not excluded by LEP. For the three values of $\tan\beta$ shown in the plots, the physical Higgs mass plotted is the second lightest Higgs, while the lightest one is a dominantly singlet Higgs with a very weak coupling to the Z boson. In fact, a weakly coupled Higgs as light as a few GeV might have escaped detection at LEP⁴. In both models, MSSM and NMSSM,

⁴An analytical fit to the experimental results giving the constraint between the mass of the scalar Higgs and its coupling to the Z boson can be found in [9].

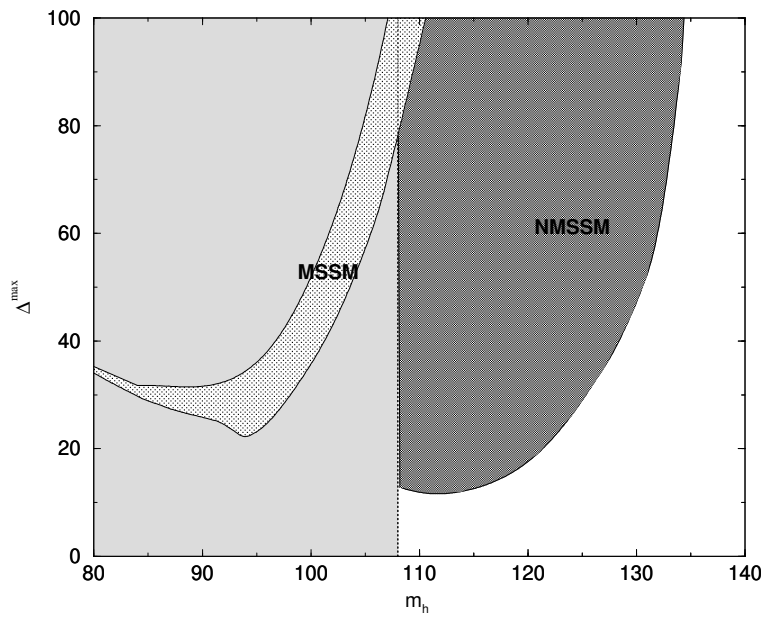


Figure 2: Same as in Fig. (1) for $\tan \beta = 3$.

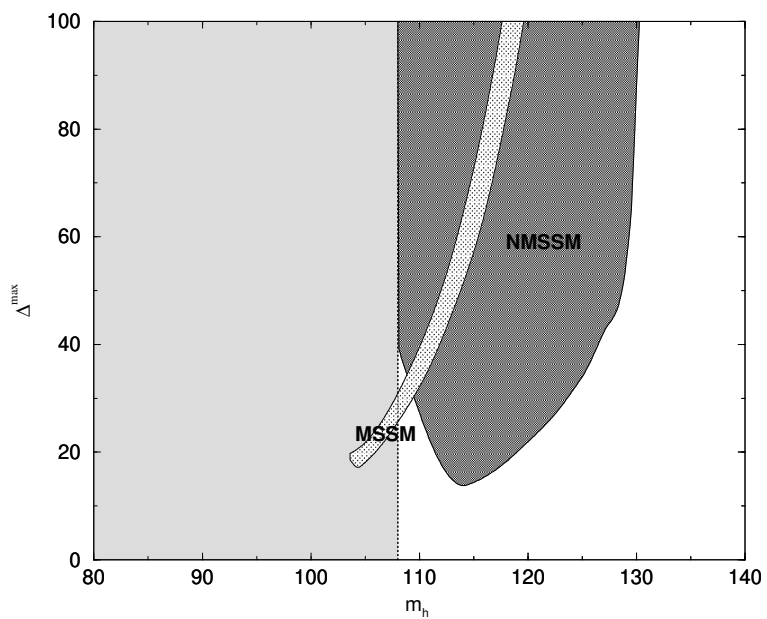


Figure 3: Same as in Fig. (1) for $\tan \beta = 5$.

the increase of the maximum fine-tuning when increasing the physical Higgs mass is mainly due to the increase in $M_3(0)$ [2]. Varying $m_{H_1}(0)$ and $m_{H_2}(0)$ has almost no effect in fine-tuning in the MSSM for values of $\tan\beta \geq 3$, and the regions obtained are narrower than in the NMSSM.

It is clear that for all three values of $\tan\beta$ the physical Higgs boson mass in the NMSSM may be heavier than in the MSSM, with correspondingly lower fine-tuning. The effect is clearly greater for lower values of $\tan\beta \leq 3$, where the experimentally allowed values of the lightest Higgs mass would imply large fine-tuning in the MSSM, whereas in the NMSSM we can have a large enough Higgs mass with a relatively low Δ^{max} . The plots are a striking demonstration that the physical Higgs boson can be heavier and involve less fine-tuning in the NMSSM compared to the MSSM at low values of $\tan\beta$.

3 Baryogenesis in the NMSSM

Having shown that the low $\tan\beta$ region of the NMSSM permits a heavier physical Higgs boson consistent with the LEP limit, without large fine-tuning, we now turn to the question of electroweak baryogenesis in the NMSSM. The anomaly mediated electroweak processes are known to provide an efficient mechanism for baryogenesis in the symmetric phase [3]. In order to prevent the washout of the resulting baryon asymmetry by the back reaction, however, one requires a strongly 1st order EWPT,

$$v_c > T_c, \quad (9)$$

where T_c is the critical temperature and v_c the Higgs VEV in the symmetry breaking phase at this temperature. This imposes serious constraints on the underlying model, since it requires a negative cubic term in the generic Higgs potential

$$V = m^2\phi^2 - \mu\phi^3 + \lambda\phi^4, \quad (10)$$

with

$$v_c = \mu/2\lambda > T_c, \quad (11)$$

where the critical point is defined as the point of degeneracy between the symmetric and symmetry breaking vacua.

In the SM, thermal loops provide a positive quadratic term as well as a negative cubic term to (10), the latter coming from the W and Z boson loops. Being a loop effect however the resulting μ is small compared to T_c , which is typically of the electroweak scale. This implies a stringent limit on λ and hence on the SM Higgs mass, $m_h \lesssim 40$ GeV [3], which is ruled out by the LEP data. In the MSSM the cubic term gets an additional contribution from stop loops; so that for a light stop ($m_{\tilde{t}_R} \sim 100$ GeV) the Higgs mass limit goes up to $m_h \lesssim 100$ GeV for $m_A \gg M_Z$ [3]. But the twin requirements on m_h and m_A squeezes the MSSM solution to the low $\tan\beta$ region, which is disfavoured by LEP. Indeed the only way of reconciling the LEP limit with the low $\tan\beta$ region is by invoking large stop mass and mixing parameters, in which case one can not satisfy (9). Thus the MSSM scenario for a strong EWPT (9) is strongly disfavoured by LEP data, if not ruled out by it altogether.

As already noted in [10, 11, 12], it is much easier to satisfy the strong EWPT requirement (9) in the NMSSM compared to the MSSM, since the tree level potential (4) itself contains a cubic term $2\lambda A_\lambda x v_1 v_2$. We closely follow the approach of [10] in using the simplest Z_3 symmetric form of the NMSSM superpotential (3) and simply retaining the leading term in the expansion of the thermal loop in M/T , i.e. the mass of the exchanged particle relative to the temperature. Thus

$$V = V_0 + V_T, \quad (12)$$

where V_0 is the zero-temperature potential represented by (4) along with the radiative

correction from top/stop loops, and

$$\begin{aligned} V_T = & \frac{T^2}{24} \left[\text{Tr } M_S^2 + \text{Tr } M_P^2 + 2m_{H^+}^2 + 6M_W^2 + 3M_Z^2 \right. \\ & \left. + 6m_t^2 + 2m_C^2 + m_{N1}^2 + m_{N2}^2 + m_{N3}^2 \right]. \end{aligned} \quad (13)$$

The last four terms represent the charged and the neutral Higgsinos. The other superparticle masses are assumed to be larger than $2T$ and hence suppressed by the Boltzmaan factor [13]. We shall evaluate the field-dependent masses of (13) in the Landau gauge as in [11] instead of the Unitary gauge of ref. [10], in view of the well-known ambiguity in calculating finite temperature effects in the latter (the so-called unitary gauge puzzle [14]). This gives [11]

$$\begin{aligned} V_T = & \frac{T^2}{24} \left[4m_{H_1}^2 + 4m_{H_2}^2 + 2m_N^2 + 2(3g^2 + g'^2 + 3\lambda^2)(v_1^2 + v_2^2) \right. \\ & \left. + 6h_t^2 v_2^2 + 12(\lambda^2 + k^2)x^2 \right]. \end{aligned} \quad (14)$$

To get the potential as a function of the Higgs fields H_1, H_2, N one has to simply substitute these quantities for their VEVs v_1, v_2, x in eqs. (4) and (14).

For a given $\tan\beta$ and stop mass and mixing parameters we first minimize the $T = 0$ potential (4) along with the radiative correction and impose the experimental constraints on the output Higgs parameters to find an appropriate set of $\lambda, k, A_\lambda, A_k$ and x parameters. We then find the T_c as the largest T at which the curvature (second derivative) of the potential changes sign along any direction at the origin. It is clear from eqs. (4), (5), (12) and (14) that

$$T_c^2 = \text{Max} \left[\frac{-12m_{H_1}^2}{3g^2 + g'^2 + 3\lambda^2}, \frac{-12(m_{H_2}^2 + \Delta_{\text{rad}})}{3g^2 + g'^2 + 3\lambda^2 + 3h_t^2}, \frac{-2m_N^2}{\lambda^2 + k^2} \right]. \quad (15)$$

where $\Delta_{\text{rad}} = \frac{-3h_t^2}{8\pi^2} m_t^2 \ell n \frac{m_t}{m_t}$ along with a stop mixing contribution. Although the T_c determined from this saddle point of the potential at the origin is not identical to the one determined by the above mentioned degeneracy between the two vacua, they have been shown to agree within 2% [11]. Therefore we use this T_c and minimise

the potential at this temperature to determine the corresponding VEVs⁵. Since both the doublet Higgs fields contribute to the sphaleron energy the relevant VEV for the requirement (9) is

$$v_c = \sqrt{2}(v_{1c}^2 + v_{2c}^2)^{\frac{1}{2}}, \quad (16)$$

where the factor $\sqrt{2}$ is due to the normalisation convention, $M_Z^2 = (g^2 + g'^2)(v_1^2 + v_2^2)/2$ as emphasised in [15].

The stop mass and mixing parameters are fixed at

$$m_{\tilde{t}} = 500 \text{ GeV}, \quad A_t = 1000 \text{ GeV}, \quad (17)$$

and input values of $\tan \beta$ are taken as 2, 3, 5 and 10. For each $\tan \beta$ we run the program at 7×10^5 points, corresponding to 7 different starting points in the parameter space. Only about 0.1% of these points give solutions satisfying the experimental constraints along with the requirement that in each case the solution represents the absolute minimum of the potential. This is about an order of magnitude less than the passing rate of ref. [11], which could be due to our using the most constrained (\mathbb{Z}_3 symmetric) form of the NMSSM as well as the stronger experimental constraints coming from LEP now. About 10% of these solutions satisfy the strong EWPT criterion (9). Thus for each of the 7 starting points in the parameter space we have $\lesssim 10$ solutions satisfying all these criteria.

Table 1 shows two representative solutions for each $\tan \beta$ along with the corresponding parameter values as well as the output Higgs boson masses, v_c and T_c . One of the solutions corresponds to a relatively low value of the lightest scalar mass, escaping the LEP constraint because of its large ($\geq 98\%$) singlet content, while the other has a lightest scalar mass above the LEP limit. We see from this table that it is possible to get acceptable Higgs mass spectra as well as satisfy $v_c > T_c$ with reasonable

⁵Our minimisation code for the NMSSM potential at finite temperature is based on the corresponding code of Manuel Drees for the zero temperature case.

$\tan \beta$	m_{Si} (GeV)	m_{Pi}, m_{H^+} (GeV)	λ, k	A_λ, A_k (GeV)	x (GeV)	v_c, T_c (GeV)
2	82,114,468	235,461,464	.33,-.12	-340,227	621	80,76
	113,139,664	390,659,662	.31,-.14	-465,379	953	162,58
3	97,126,751	145,750,747	.48,-.12	-658,94	485	118,81
	115,126,975	169,977,973	.41,.10	-1067,-146	704	187,61
5	46,127,618	84,620,614	.43,.12	-690,-107	257	191,66
	122,166,606	296,604,609	.14,-.15	-510,243	798	123,82
10	109,127,456	146,455,462	.04,-.10	-737,102	709	110,91
	120,128,844	187,844,847	.12,.14	-1082,-145	583	156,78

Table 1: Representative sample of NMSSM solutions satisfying all the experimental constraints along with the requirement of a strong EWPT ($v_c > T_c$). The physical Higgs masses are shown along with the model parameters. ($m_{\tilde{t}} = 500$ GeV, $A_t = 1000$ GeV).

values of the parameters, at least for low values of $\tan\beta$ (2,3,5). Interestingly one gets acceptable solutions for $\tan\beta = 10$ as well; but in this case $k > \lambda$. The reason is that for large $\tan\beta$ the 3rd and 4th terms of the potential (4) become vanishingly small. The latter implies that the m_h^2 limit of eq. 2 is dominated by the 1st term, which is however quite large now; while the former implies that the dominant cubic term of the potential is $\frac{2}{3}kA_kx^3$. Thus the NMSSM can help to get a strong EWPT in the large $\tan\beta$ region as well, where it has little effect on the Higgs mass limit of the MSSM.

It is appropriate to briefly discuss here the role of NMSSM in generating sufficient amount of CP asymmetry, as required for baryogenesis [15, 16]. Of course quantitative investigation of this question depends on the model of electroweak baryogenesis, which is beyond the scope of this work. But it is generally agreed that the size of CP violation in the SM, arising from the complex CKM matrix, is much too small as it is suppressed by the small Yukawa couplings as well as the CKM mixing angles. There are additional sources of CP violation in the MSSM, arising from the phases of μ and the SUSY breaking terms, which can serve this purpose provided the size of the phase angles are $\geq O(10^{-1})$ [3]. On the other hand the experimental constraint from the electric dipole moments of neutron and electron would require these phase angles to be $\leq O(10^{-2})$ unless there is a systematic cancellation between them [17] or one assumes the sfermions of the 1st two generations to have masses $\gg 1$ TeV [18]. This potential conflict with the electric dipole moment limits is alleviated in the NMSSM, where the required size of phase angles is an order of magnitude smaller than in MSSM [15]. Even more interestingly the NMSSM offers the possibility of generating a spontaneous CP violation in the symmetric phase, which goes down to zero in the symmetry breaking phase [15, 16]. Thus it can effectively contribute to baryogenesis, which takes place in the symmetric phase, while making no contribution to the measured electric dipole moments. It is not possible to generate such a transitional CP violation

in the MSSM [15].

4 Conclusion

The current LEP limit on the lightest Higgs boson mass places severe constraints on the MSSM in the low $\tan\beta$ region, which was the favoured region for a strong EWPT as required for electroweak baryogenesis. The only way to escape this m_h limit is to invoke very large stop mass and mixing parameters, which would imply however large fine-tuning as well as a weak EWPT. Thus one has to sacrifice the naturalness of electroweak symmetry breaking as well as baryogenesis. However both these problems can be solved simultaneously with the so called μ problem of the MSSM by going to the NMSSM. All the relevant terms – i.e. $\lambda^2 x^2 v_{1(2)}^2$, $\lambda^2 v_1^2 v_2^2$ and $\lambda A_\lambda x v_1 v_2$ – originate from the superpotential $\lambda N H_1 H_2$. While the 1st term solves the so-called μ problem, the 2nd provides an additional contribution to the tree-level m_h limit and the 3rd one a cubic term in the tree-level potential. Thus the 2nd term alleviates the fine-tuning problem arising from the m_h limit, while the 3rd ensures a strong EWPT.

It may be noted here that both the 2nd and the 3rd terms vanish at large $\tan\beta$. Thus it does not affect the m_h limit of the MSSM at large $\tan\beta$, which is any way quite high. However in this case the soft cubic term $k A_k x^3$ helps to generate a strong EWPT. Thus the NMSSM helps to give a strong EWPT along with solving the μ problem even in the large $\tan\beta$ region.

To summarise, the LEP limit on the Higgs boson mass severely constrains the low $\tan\beta$ region of the MSSM, leading to large fine-tuning and problems with electroweak baryogenesis. We have shown that in the low $\tan\beta$ region the NMSSM is in much better shape phenomenologically, since the physical Higgs boson masses are larger, the fine-tuning is less, and the electroweak phase transition is more strongly first order in the NMSSM, as compared to the MSSM.

Acknowledgements

The authors would like to thank the organisers of WHEPP-6, where this project was started, and B. Ananthanarayan and P.N. Pandita for their contributions during the initial stage of the work. We would also like to thank C.D. Froggatt and M. Pietroni for several helpful communications.

References

- [1] J.F. Grivaz, Plenary talk at the WHEPP-6, Chennai, India (3-14 January, 2000);
A. Sopczak, hep-ph/0004015.
- [2] G.L. Kane, S.F. King, *Phys. Lett.* **B 451** (1999) 113;
M. Bastero-Gil, G.L. Kane, S.F. King, *Phys. Lett.* **B 474** (2000) 103.
- [3] For a review and references to earlier works see, e.g.:
M. Carena, C.E.M. Wagner, in *Perspectives on Higgs Physics II*, ed. G.L. Kane, World-Scientific, Singapore (1998);
J. Cline, Plenary talk at the WHEPP-6, Chennai, India (3-14 January, 2000)
hep-ph/0003029.
- [4] M. Brhlik, G.J. Good, G.L. Kane, hep-ph/9911243.
- [5] P. Fayet, *Nucl. Phys.* **B 90** (1975) 104;
H.P. Nilles, M. Srednicki, D. Wyler, *Phys. Lett.* **B 120** (1983) 346;
J.P. Derendinger, C.A. Savoy, *Nucl. Phys.* **B 237** (1984) 307;
J. Ellis, J.F. Gunion, H.E. Haber, L. Roszkowski, F. Zwirner, *Phys. Rev.* **D 39** (1989) 844;
L. Durand, J.L. Lopez, *Phys. Lett.* **B 217** (1989) 463;
M. Drees, *Int. J. Mod. Phys.* **A 4** (1989) 3635.

- [6] U. Ellwanger, *Phys. Lett.* **B 303** (1993) 271;
 U. Ellwanger, M. Rausch de Traubenberg, C. A. Savoy, *Phys. Lett.* **B 315** (1993) 331, *Z. Phys.* **C 67** (1995) 665, *Nucl. Phys.* **B 492** (1997) 21;
 T. Elliott, S.F. King, P.L. White, *Phys. Lett.* **B351** (1995) 213;
 S. F. King, P. L. White, *Phys. Rev.* **D52** (1995) 4183; M. Drees, E. Ma, P.N. Pandita, D.P. Roy, S. Vempati, *Phys. Lett.* **B 433** (1998) 346.
- [7] C. Panagiotakopoulos, K. Tamvakis, *Phys.Lett.* **B 446** (1999) 224.
- [8] R. Barbieri, G.F. Giudice, *Nucl. Phys.* **B 306** (1988) 63.
- [9] U. Ellwanger, C. Hugonie, hep-ph/9909260 (to appear in *Eur. Phys. J. C*).
- [10] M. Pietroni, *Nucl. Phys.* **B 402** (1993) 27.
- [11] A.T. Davies, C.D. Froggatt, R.G. Moorhouse, *Phys. Lett.* **B 372** (1996) 88.
- [12] S.J. Huber, M.G. Schmidt, *Eur. Phys. J. C* **10** (1999) 473.
- [13] L. Dolan, R. Jackiw, *Phys. Rev.* **D 9** (1974) 3320.
- [14] P.F. Kelly, R. Kobes, G. Kunstatter, *Phys. Rev.* **D 50** (1994) 7592.
- [15] S.J. Huber, M.G. Schmidt, hep-ph/0003122.
- [16] D. Comelli, M. Pietroni, A. Riotto, *Phys. Rev.* **D 50** (1994) 7703.
- [17] T. Ibrahim, P. Nath, *Phys. Rev.* **D 58** (1998) 111301.
- [18] Y. Kizukuri, N. Oshimo, *Phys. Rev.* **D 45** (1992) 1806.